Adsorption Science & Technology

Article

Adsorption of peroxidase from *Raphanus sativus* L onto alginate–guar gum matrix: Kinetic, equilibrium and thermodynamic analysis

Adsorption Science & Technology
2016, Vol. 34(6) 388–402

DOI: 10.1177/0263617416659287
adt.sagepub.com

SAGE

Ana C Santos Leite da Silva
Institute of Biotechnological and Chemistry Processes, Faculty of Biochemical and Pharmaceutical Sciences and CONICET, National University of Rosario, Rosario, Argentina; Centre of Biological Engineering, University of Minho, Braga, Portugal

Nadia Woitovich Valetti
Institute of Biotechnological and Chemistry Processes, Faculty of Biochemical and Pharmaceutical Sciences and CONICET, National University of Rosario, Rosario, Argentina

María E Brassesco
Institute of Biotechnological and Chemistry Processes, Faculty of Biochemical and Pharmaceutical Sciences and CONICET, National University of Rosario, Rosario, Argentina

José A Teixeira
Centre of Biological Engineering, University of Minho, Braga, Portugal

Guillermo Picó
Institute of Biotechnological and Chemistry Processes, Faculty of Biochemical and Pharmaceutical Sciences and CONICET, National University of Rosario, Rosario, Argentina

Abstract

This work explores the kinetics, equilibrium and thermodynamics of peroxidase adsorption onto spherical guar gum–alginate matrices. The effect of contact time, solution pH, initial protein concentration and temperature was studied in batch experiments. The results show that peroxidase adsorption increased with rising contact time and initial enzyme concentration, and was higher at pH 4.0. The kinetic processes can be predicted by both the pseudo-first-order rate kinetics and the pseudo-second-order rate kinetics. Equilibrium adsorption data were analyzed with different isotherm models. The experimental data fitted to the Freundlich model in

Corresponding author:
Guillermo Picó, Faculty of Biochemical and Pharmaceutical Sciences, Nacional University of Rosario, Suipacha 570, (S2002RLK) Rosario, Argentina.
Email: gpico@fbioyf.unr.edu.ar

agreement with the low energy activation, demonstrating the presence of a high physical and unspecific interaction between the enzyme and the matrix.

Keywords
Alginate, guar gum, polyelectrolytes, peroxidase, adsorption, isotherms

Introduction

Adsorption is defined as the ability of some materials (biomass, biological material, polymers, inorganic solids, etc.) to bind solutes present in aqueous solution. Adsorption is a complex physicochemical process, which includes many steps such as diffusion of the solute through the boundary layer, intra-particle diffusion and adsorption of the solute on the sorbent surface. There are countless studies about using different biomass wastes from vegetal or microbiological origin, as substitutes to the expensive and more conventional use of activated carbon, in the adsorption mechanism to remove heavy metal and different toxic components from liquid wastes (Dotto et al., 2012; Pardo et al., 2003; Rangabhashiyam et al., 2014). At present adsorption has emerged as an eco-friendly alternative technology to remove several molecules from aqueous solutions (Zhang et al., 2013). This technology has numerous advantages, such as, its simplicity, being easy to do, using environmentally friendly components and having non-expensive preparation methods of the adsorbent (Gadd, 2009). Much attention has been given to the obtainment of non-soluble matrices formed by polysaccharides and natural polyelectrolytes such as alginate, chitosan, carrageenan, etc. (Gotoh et al., 2004; Kulkarni et al., 2000; Roy et al., 2005; Somers et al., 1993; Spelzini et al., 2011; Woitovich Valetti and Picó, 2016).

Sodium alginate (Alg) is a particularly attractive biopolymer that has a wide range of applications, particularly, in the biomedicine, industrial, food and pharmaceutical fields, because of its capacity to hold water, form gels and form stable emulsions. Alg is a water-soluble linear, polysaccharide composed of 1,4-linked β-D-mannuronicand α-L-glucuronic acid residues, which are found in varying composition and sequence (Lee and Mooney, 2012). This polymer has the advantage of being of natural origin, having a friendly behaviour when it is discarded in the environment and being low-priced. The gelation of Alg can be carried out under an extremely mild environment using non-toxic reactants. The most important property of Alg is its ability to form gels by reaction with divalent cations. Alg beads can be prepared by extruding a solution of Alg as droplets into a divalent cations solution such as Ca^{2+} or Ba^{2+} (Paques et al., 2014). There are a great number of papers where Alg is transformed into a non-soluble matrix adding Ca^{2+} to the medium (Daly and Knorr, 1988; Spelzini et al., 2011). However, the working pH range of the matrix is limited and when Ca^{2+} is lost by the matrix, the Alg–calcium complex is destroyed, being the polymer soluble (López-Morales et al., 2013). The spherical matrix is permeable to small molecules and macromolecules and they can interact with it by difference in their electrical charge. So this matrix can act as an ionic exchange adsorbent of different molecules. However, the matrices of Alg have a limited capacity, which depends in part of its porosity and the distance between the polymer chains.

Guar gum (GG) is a non-ionic polysaccharide found abundantly in nature and has many properties desirable for drug delivery applications. However, due to its high swelling

characteristics in aqueous solution, the use of GG as delivery carriers is limited. GG is a water soluble polysaccharide derived from the seeds of *Cyamopsis tetragonolobus*, family *Leguminosae* (Mudgil et al., 2014). GG is comprised of a high molecular weight polysaccharides composed of galactomannans consisting of a (1-4)-linked β-D-mannopyranose backbone with branch points from their 6-positions linked to α-D-galactose (Yoon et al., 2008). GG is used as a thickener in cosmetics, sauces, salad dressings and as an agent in ice cream, which prevents formation of ice crystals. In pharmaceutical formulations, it is used as a binder and disintegrator in solid dosage forms, and as a suspending, thickening and stabilizing agent in liquid formulations (Mudgil et al., 2014).

Alg–GG beads are not very stable, but the cross-linked Alg–GG matrix showed stability over a wide pH range and also in the presence of phosphate or Ca^{2+} chelator (Roy et al., 2005).

The goal of this work was to analyse the molecular mechanism of adsorption of a model protein as peroxidase onto a matrix formed by Alg and GG cross-linked with epichlorohydrin to provide stability. To achieve this goal, we have determined the kinetics mechanism and isotherms of adsorption together with thermodynamic variables.

Materials and methods

Chemical

Alginic acid sodium salt (Alg), GG, epichlorohydrin and peroxidase from *Raphanus sativus* L (POD) were purchased from Sigma-Aldrich and used without further purification. All other reagents were also of analytical grade. The solutions were prepared with distilled water.

Preparation of Alg–GG beads

One hundred twenty-five milligrams of GG were dissolved in 25 mL of distilled water. Alg–GG beads with distinct Alg to GG percentage weight ratios were prepared (0.6:0.5, 1.0:0.5, and 1.5:0.5). Alg was dissolved in the GG solution prepared as above, and left stirring until complete dissolution. Beads were formed by dropping this solution through a syringe into a 50 mL of 0.1 M $CaCl_2$ solution according to the method previously reported (Roy et al., 2005). The beads were maintained in stirring overnight and finally incubated in 6 mM $CaCl_2$ solution at 5°C.

Preparation of non-soluble Alg–GG beads

Cross-linked Alg–GG particles were prepared by adapting the procedure of Roy et al. (2005). Alg–GG beads (5 g) were transferred to absolute ethanol containing 0.1 M $CaCl_2$ (25 mL) and incubated for 30 min at 45°C. To this 1.5 mL or 3 mL of epichlorohydrin was added in small aliquots and were kept for 10 min stirring constantly. To this 4.2 mL and 8.4 mL, respectively, of 5 N NaOH were added and kept overnight at 30°C. Finally, acetic acid was added to the system until the pH became neutral. The cross-linked Alg–GG beads thus formed were washed with 30 mL of a 3:1 mixture (v/v) of absolute ethanol and water, followed by 20 mL of 99% ethanol. The matrix was finally re-suspended in distilled water and equilibrated with the work buffer before use.

To check the intersection of matrices we combine a certain amount of 0.1 M EDTA, which binds strongly to Ca^{2+}. EDTA forms complex with the Ca^{2+} present in the sample, and if the cross-linking was not successful the cation loss leads to the dissolution of the beads.

Measurement of enzymatic activity of POD

POD activity was spectrophotometrically monitored by following the oxidation of pyrogallol to purpurogallin. The reaction mixture is: 300 µL of pyrogallol 21.32% (w/v), 200 µL of H_2O_2 8 Vol, 2.40 mL 100 mM phosphate buffer pH 6.0 and sufficient enzyme to give a considerable change in the 420 nm absorbance between 0 and 90 seconds. The slope of the initial linear portion of the absorbance vs. time curve is proportional to the POD activity. Measurements were taken every 0.1 s and the solution remained under continuous agitation during the measurements. The activity of POD was calculated by the following equation:

$$UA_{\mathrm{POD}} = \frac{(\Delta \mathrm{Abs}_{420\mathrm{nm_s}} - \Delta \mathrm{Abs}_{420\mathrm{nm_b}}).V_{\mathrm{a}}.d_{\mathrm{f}}}{12.V_s} \quad (1)$$

where: $\Delta \mathrm{Abs}_{420\mathrm{s}}$ and $\Delta \mathrm{Abs}_{420\mathrm{b}}$ are the absorbance changes at 420 nm for the sample and the blank, respectively, V is the total volume of assay, V_s is the sample volume, d_f is the dilution factor (V_s/V_a) and 12 is the extinction coefficient of 1 mg/mL of purpurogallin at 420 nm.

Determination of total protein concentration

It was carried out using the Bicinchoninic assay. A fresh standard working reagent (SWR) was prepared mixing 98 Vol of reagent A (Bicinchoninic acid solution purchased from Sigma Aldrich) and 2 Vol of reagent B ($CuSO_4$ solution 4% w/v). A volume of 10 µL of protein solution (maximum concentration of 1 mg/mL) was added to 1 mL of SWR. The tubes were incubated at 37°C for 30 min. After leaving them to cool down at room temperature, the absorbance was measured at 562 nm using a cell with a 1 cm path length. The calibration curve was performed using dilutions of a standard solution of BSA 1 mg/mL.

Determination of adsorption conditions

The batch experiments for the adsorption kinetics of commercial POD onto cross-linked Alg–GG beads were carried out measuring the enzymatic activity of free POD in the supernatant over time. The mixtures were prepared with constant activity of POD in 25 mM sodium acetate buffer at different pH (4.0, 5.0 and 5.5) and stirring constantly at 20 rpm until the adsorption equilibrium was reached.

Adsorption kinetics

To analyze the adsorption kinetic mechanism the adsorbed POD amounts vs. time curves were fitted with two models, namely pseudo-first- and pseudo-second-order. The kinetic adsorption was assayed at two temperatures and at three different initial concentrations of enzyme. The mixtures were prepared with constant activity of POD in 25 mM sodium acetate buffer, pH 4.0 and stirring constantly at 20 rpm until the adsorption equilibrium was reached.

Adsorption isotherms

Adsorption isotherm of POD was determined by equilibrating different quantities of POD with 100 mg cross-linked Alg–GG beads at pH 4.0 and two temperatures: 25°C and 6°C. The mixtures were stirred until the adsorption equilibrium was reached and free protein in the supernatant was determined. The amount of POD adsorbed at equilibrium time by unit of mass adsorbent (m) was determined by the following equation:

$$\frac{UA_{\mathrm{POD_{Adsorbed}}}}{mg_{\mathrm{matrix}}} = \frac{UA_{\mathrm{POD_i}} - UA_{\mathrm{POD_f}}}{m_{\mathrm{matrix}}} \tag{2}$$

where UA_{PODi} is the initial activity of POD in the system; UA_{PODf} is the POD activity in supernatant after adsorption equilibrium was reached and m_{matrix} is the mass in grams of adsorbent in the system. The UAs were calculated following equation (1). Results were expressed as $UA_{\mathrm{ads}}/mg_{\mathrm{matrix}}$ vs. UA_{eq}/mL.

Thermodynamic evaluation

The thermodynamic state functions (free energy, enthalpy and entropy) are important indicators when estimating the mechanism of adsorption process. The distribution coefficient (K_0) reflects the binding ability of the surface for a molecule. The K_0 is defined as follow:

$$K_0 = \frac{C_{\mathrm{s}}}{C_{\mathrm{eq}}} \tag{3}$$

where C_{s} is the quantity of POD adsorbed in the solid matrix (mg/g) and C_{eq} is the quantity of free POD in solution in equilibrium with the POD adsorbed (mg/mL). K_0 can be obtained from extrapolating C_{eq} to zero in the plots of $\ln(C_{\mathrm{s}}/C_{\mathrm{eq}})$ vs. C_{eq} at both temperatures (Zhang et al., 2013).

The standard Gibbs energy (ΔG°), enthalpic (ΔH) and entropic changes (ΔS°) were estimated by applying the thermodynamic equation as follows:

$$\Delta G^{\circ} = -RT\ln K_0 \tag{4}$$

$$\ln\frac{K_{0.298}}{K_{0.281}} = \frac{\Delta H^{\circ}}{R}\left(\frac{1}{281} - \frac{1}{298}\right) \tag{5}$$

$$\Delta G^{\circ} = \Delta H^{\circ} - T\Delta S^{\circ} \tag{6}$$

where R is the universal gas constant ($8.314 \times 10^{-3}\,\mathrm{kJ\,mol^{-1}\,K^{-1}}$), T is the absolute temperature in Kelvin and K_0 is the distribution coefficient of the enzyme between the adsorbed layer and the solution at the corresponding temperature.

Data analysis

Nonlinear regression analysis was applied to estimate the isotherm and kinetic model parameters. Nonlinear regression was performed using trial and error method with the help of Sigma Plot v11 software. In trial error procedure, isotherm and kinetic parameters

were estimated by maximizing the coefficient of determination (R^2) (sum of squares) and minimizing the value of SS (least sum of squares). Both coefficients have been widely employed to measure the fitting degree of model to adsorption data (Woitovich Valetti and Picó, 2016). The coefficients were calculated according to the following equations:

Least sum of squares:

$$SS = \sum (q_c - q)^2 \tag{7}$$

The R^2 coefficient:

$$R^2 = \frac{\sum (q_{mod} - q_{exp})^2}{\sum (q_{mod} - q_{aexp})^2 + (q_{mod} - q_{exp})^2} \tag{8}$$

Results and discussion

Determination of best adsorption conditions

In order to determine the matrix composition that has the major adsorption capacity, different variables were studied: the initial concentration of alginate, while maintaining constant the total concentration of GG, the concentration of epichlorohydrin and pH. The criteria used to choose the optimal matrixes were: non-solubility of the matrix in the presence of Ca^{2+}, capacity of adsorption of POD and pH effect on it. Table 1 shows the results obtained; it can be seen that the matrix formed by 0.6%, 1.0% and 1.5% (w/v) of Alg and cross-linked with 1.5 and 3.0 mL of epichlorohydrin at pH between 4.0 and 5.5 were suitable to adsorb POD. However, the pH effect shows that the maximal capacity of adsorption was at pH 4.0. The following systems were chosen: S1: 0.6% (w/v)Alg–0.5% (w/v) GG; S2: 1% (w/v)Alg–0.5% (w/v) GG and S3: 1.5% (w/v) Alg–0.5% (w/v) GG. From the different combinations of Alg–GG tested, the 1.0:0.5 and 1.5:0.5 combinations were found to be the most suitable (S2 and S3). Table 1 allows us to discard the systems that adsorb at pH 5.0 and 5.5, because the adsorbed percent of POD was low. At pH 4.0, the S2 and S3 with 1.5 mL epichlorohydrin showed a good capacity of adsorption, so we have chosen these two systems to carry out the following adsorption experiments.

These results can be explained taking into account the electrical charge of POD and Alg. Generally, commercial Alg have a pKa of 3.2; therefore posses negative charge at pH higher than 3.2. POD isoenzymes posses an isoelectrical pH of 5.5. At pH lower than 5.5 the positively charged groups of POD interact with the negatively charged groups present in Alg resulting in adsorption. The best pH for adsorption is 4.0 since in this value the opposite charges present in the enzyme and polymer are higher. On the other hand, it was expected that a higher concentration of Alg in the matrix increases its ability to interact electrostatically with the enzyme due to the presence of more charges for interact.

Kinetic studies

The kinetic of adsorption was assayed at two temperatures and at three different initial amounts of POD (Figure 1). It can be seen that the adsorbed protein increases with the contact time until it reaches a plateau. The point where the plateau begins is the equilibrium time required to achieve the maximum adsorption in these conditions. A relatively rapid

Table 1. Adsorption of POD expressed as percent (%) on the initial POD activity in function of pH, using the matrix system 1, 2 and 3.[a]

% (w/v) Alg	Epichlorohydrin (mL)	pH	Adsorption of POD (%)
0.6	1.5	4.0	70
1.0			81
1.5			85
0.6	3.0		58
1.0			47
1.5			83
0.6	1.5	5.0	31
1.0			34
1.5			48
0.6	3.0		16
1.0			17
1.5			43
0.6	1.5	5.5	8
1.0			11
1.5			1
0.6	3.0		0
1.0			0
1.5			0

[a]The concentration of GG was 0.5% (w/v), temperature 21°C and medium 25 mM sodium acetate buffer. Total amount of Alg–GG matrix 100 mg.

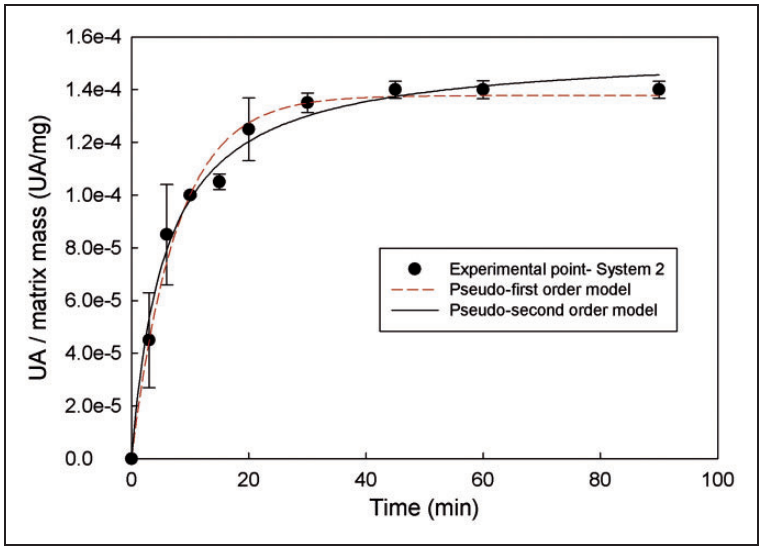

Figure 1. Kinetics of POD adsorption on the Alg–GG matrix S2. Medium: 25 mM sodium acetate buffer, pH 4.0. Total amount of Alg–GG matrix 100 mg. Total amount of POD 0.01564UA. Temperature 21°C. (Results from S3 system are similar – data not shown.)

uptake and establishment of equilibrium in a short time indicate the efficacy of that adsorbent for its use in protein absorption from a biomass solution. Available adsorption studies in literature reveal that the uptake of adsorbate species is fast at the initial stages of the contact period, and thereafter, it becomes slower near the equilibrium (Chiou et al., 2004; Woitovich Valetti and Picó, 2016). Between these two stages of the uptake, the rate of adsorption is found to be nearly constant. This is obvious from the fact that a large number of vacant surface sites are available for adsorption during the initial stage, and after a lapse of time, the remaining vacant surface sites are difficult to be occupied due to repulsive forces between the solute molecules on the solid and bulk phases (Luo et al., 2013).

To analyze the adsorption kinetic mechanism, the experimental data at different temperatures and concentrations were fitted with two models, namely pseudo-first-order and pseudo-second-order, respectively as shown in equations (9) and (10).

$$q_t = q_e(1 - e^{-k_1 t}) \tag{9}$$

where q_t and q_e (UA/mg) are the amounts of POD adsorbed per unit weight of matrix in a time t and at the equilibrium respectively, and $k_1(\text{min}^{-1})$ is the constant rate of pseudo-first-order adsorption.

$$q_t = \frac{k_2 q_e^2 t}{1 + k_2 q_e t} \tag{10}$$

where q_t and q_e (UA/mg) are the amounts of POD adsorbed per unit weight of matrix in a time t and at the equilibrium, respectively, and k_2 (g/mg min) is the constant rate of pseudo-second-order adsorption.

The parameter values obtained from the kinetic models and the regression correlation coefficients (R^2) are listed in Table 2. The calculated correlation coefficient values for first-order- (0.9847–0.9885) and second-order- (0.9834–0.9880) kinetics were found to be greater than 0.9000, which shows the applicability of both these kinetic models. Thus, in the present both the pseudo-first-order and pseudo-second-order kinetic expressions can predict the kinetic processing experimental condition.

Table 2. Kinetic parameters of adsorption of POD onto Alg–GG beads.[a]

System	T (°C)	k_1 (min^{-1})	R^2	SS	k_2 (g $\text{mg}^{-1}\,\text{min}^{-1}$)	R^2	SS	ΔE_a kJ/mol
2	21	$(1.293 \pm 0.111) \times 10^{-1}$	0.9847	3.049×10^{-10}	1120.17 ± 155.98	0.9880	2.393×10^{-10}	42.0
2	6	$(5.08 \pm 0.45) \times 10^{-2}$	0.9875	1.072×10^{-10}	441.42 ± 83.37	0.9880	1.023×10^{-10}	
3	21	$(5.71 \pm 0.47) \times 10^{-2}$	0.9885	1.901×10^{-10}	384.61 ± 74.57	0.9861	2.300×10^{-10}	36.0
3	6	$(2.89 \pm 0.32) \times 10^{-2}$	0.9884	9.096×10^{-11}	175.65 ± 61.46	0.9834	1.298×10^{-10}	

[a]Medium: 25 mM sodium acetate buffer, pH 4.0. The initial total amount of POD is constant in all the systems. Temperature 21°C and 6°C.

Intra-particle diffusion mechanism

The solute transfer is usually characterized by either external mass transfer (boundary layer diffusion), intra-particle diffusion or both. The sorption dynamics can be described by the following three consecutive steps which are as follows (Vadivelan and Kumar, 2005):

- Transport of the solute from bulk solution through liquid film to the adsorbent surface;
- Solute diffusion into the pore of adsorbent except for a small quantity of sorption on the external surface; parallel to this is the intra-particle transport mechanism of the surface diffusion;
- Sorption of solute on the interior surfaces of the pores and capillary spaces of the adsorbent.

The third step is assumed to be rapid and considered to be negligible. The overall rate of sorption will be controlled by the slowest step, which would be either film diffusion or pore diffusion. The most commonly used technique for identifying the mechanism involved in the sorption processes by fitting the experimental data in an intra-particle diffusion plot. Previous studies by various researchers (Daneshvar et al., 2012; Vadivelan and Kumar, 2005) showed that the plot of Q_e vs. $t^{0.5}$ represents multilinearity, which characterizes the two or more steps involved in a sorption process. The intra-particle diffusion model is given in a simplified form by (Daneshvar et al., 2012):

$$Q_e = K_{id} t^{0.5} + C \tag{11}$$

where K_{id} is the intra-particle diffusion coefficient (mg/g min$^{0.5}$) and C is a constant related to the extent of the boundary layer effect. Thus the K_{id} (mg/g min$^{0.5}$) value can be obtained from the slope of the plot of Q_e (mg/g) versus $t^{0.5}$ (min$^{0.5}$) as shown in Figure 2. It was noted that the sorption process tends to be followed by two phases. It was found that the linear portion ended with a smooth curve followed by a linear portion. The two phases in the intra-particle diffusion plot suggest that the sorption process proceeds by surface sorption and intra-particle diffusion. The initial curved portion of the plot indicates a boundary layer effect while the second linear portion is due to intra-particle or pore diffusion. The slope of the second linear portion of the plot (near the saturation of the surface) has been defined as the intra-particle diffusion parameter K_{id} (mg/g min$^{0.5}$), while intercept of the plot reflects the boundary layer effect (the C constant) (Doğan and Alkan, 2003). The larger the interception, greater is the contribution of the surface sorption in the rate-limiting step. It can be seen that the increase in total initial POD concentration increases the enzyme diffusion, however, the S2 showed significant minor values in agreement with a low attraction of the matrix for the protein, due to its minor electric density. As the double nature of intra-particle diffusion plot confirms the presence of both film and pore diffusion, in order to predict the actual slow step involved. According to the first step (fast one) covering the time range between 4 and 8 min, the adsorption of POD onto Alg–GG is a surface phenomenon attributing to diffusion of the enzyme through the film solution to the external surface of the matrix. The last step (the slower and rate determining) is the gradual adsorption limited by diffusion of solute in the liquid contained in pores of the adsorbent particles and along the pores.

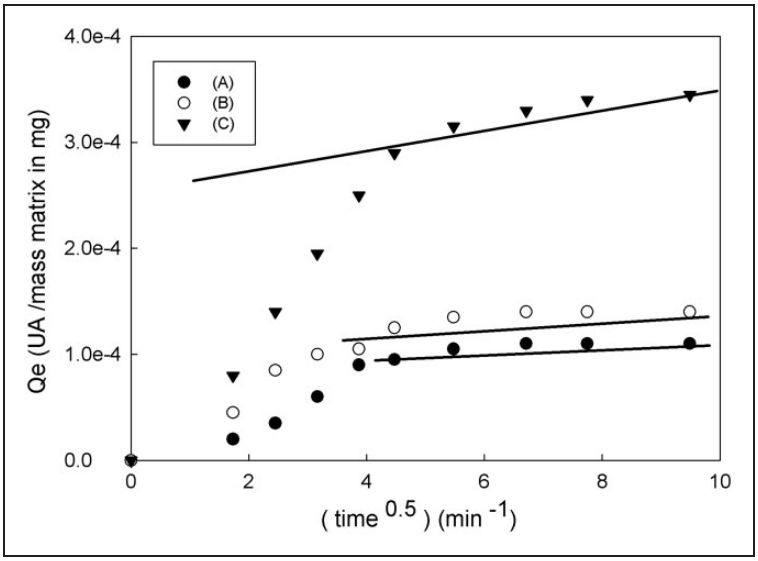

Figure 2. Intra-particle diffusion plot for POD onto Alg–GG matrices S2 (at different initial total concentration of POD), the data have been taken from Figure 1. All the other conditions are the same as Figure 1. The total POD amounts were: A: 0.0134UA, B: 0.0156UA and C: 0.0405UA. (Results from S3 system are similar – data not shown.)

The relationship between the pseudo-second-order rate constant K_2 and temperature can be calculated using the Arrhenius equation as shown in equation (12).

$$\ln K_2 = A_0 \exp \frac{-E_a}{\mathrm{RT}} \tag{12}$$

where A_0 is the temperature independent factor called 'frequency factor', R is the universal gas constant (8.314 kJ $\mathrm{mol}^{-1}\,\mathrm{K}^{-1}$), T is the absolute temperature (K) and E_a is the sorption activation energy (kJ mol^{-1}) (Bai et al., 2013). Magnitude of E_a may give an idea about the type of sorption. Two main types of adsorption may occur, physical and chemical. In physical adsorption the equilibrium is usually rapidly attained and easily reversible, because the energy barrier is low. The activation energy for physical adsorption is usually no more than 50 kJ mol^{-1}, since the forces involved in physical adsorption are of the type of Van der Walls or weak dipole–dipole interaction. From the above analysis, it can be concluded that POD adsorption by the two systems was a physical sorption process.

Isotherm modelling

Equilibrium adsorption isotherms are known to be very important when it comes to understanding the mechanisms of the adsorption and describing how adsorbates interact with adsorbents. We performed the isotherm absorption at pH 4.0 because this pH value was found to be optimal to perform the adsorption process, so, the temperature effect on the adsorption was analysed. By visual inspection of the adsorption isotherm experimental data (Figure 3), a poor adsorption of enzyme at low protein concentration can be seen, but at

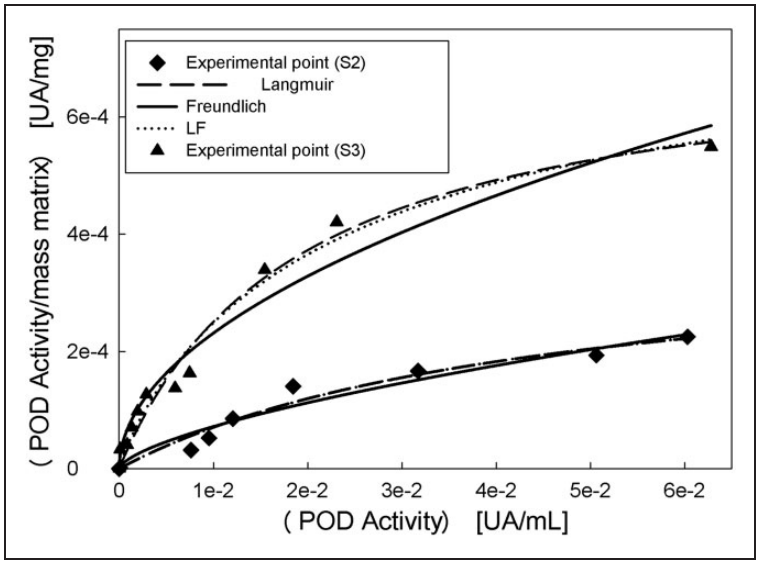

Figure 3. Adsorption isotherm of POD onto non-soluble Alg–GG beads S2 and S3. Medium: 25 mM sodium acetate buffer, pH 4.0. Temperature: 25°C.

increased POD total activity, the bound fraction of enzyme was significantly enhanced. S2 showed high adsorption capacity than S3 (data not shown).

To optimize the design of an adsorption system for the removal of adsorbate, it is important to establish the most appropriate correlation for the equilibrium data. Various isotherm equations have been used to describe the isotherm curve. In order to estimate the validity of isotherm models with experimental data, two-parameter equations were used namely, Freundlich and Langmuir which are given by equations (13) and (14):

$$q_e = K_F C_e^{1/n} \tag{13}$$

$$q_e = \frac{q_m K_L C_e}{1 + K_L C_e} \tag{14}$$

and three-parameter equation that combines the features of both Freundlich and Langmuir models (Mohammadi et al., 2011) (equation 15):

$$q_e = \frac{q_m K_{LF} C_e^{1/n}}{1 + K_{LF} C_e^{1/n}} \tag{15}$$

where q_e is the specific equilibrium amount of adsorbate, C_e is the equilibrium concentration of adsorbate, q_m is the maximal adsorption capacity and K (K_F, K_L and K_{LF}) and n are empirical constants that indicate the extent of adsorption and the adsorption effectiveness, respectively. Freundlich isotherm is an empirical equation used for the description of multilayer adsorption with interaction between adsorbed molecules. The Langmuir model is valid for monolayer adsorption to a surface with a finite number of identical sites. The Langmuir–Freundlich (LF) isotherm, also known as Sip's equation, is a versatile isotherm

Table 3. Isotherm constants for POD adsorption onto Alg–GG matrix.

T (°C)	System	Freundlich				
25		K^F		$1/n$	R^2	SS
	2	$(4.3 \pm 1.1) \times 10^{-3}$		$(47.8 \pm 4.6) \times 10^{-2}$	0.9738	3.747×10^{-9}
	3	$(7.3 \pm 1.5) \times 10^{-3}$		$(77.1 \pm 5.5) \times 10^{-2}$	0.9833	6.871×10^{-9}
		Langmuir				
		K_L		q_m (UA/mg$_{matrix}$)	R^2	SS
	2	576.1 ± 232.7		$(4.5 \pm 3.1) \times 10^{-4}$	0.9476	7.507×10^{-9}
	3	18.6 ± 5.3		$(13.8 \pm 5.1) \times 10^{-4}$	0.9883	4.798×10^{-9}
		Langmuir–Freundlich				
		K_{LF}	$1/n$	q_m (UA/mg$_{matrix}$)	R^2	SS
	2	3.0 ± 1.3	$(5.2 \pm 1.7) \times 10^{-1}$	$(21.5 \pm 6.9) \times 10^{-4}$	0.9742	3.687×10^{-9}
	3	18.6 ± 25.1	1.0 ± 0.2	$(13.8 \pm 8.9) \times 10^{-4}$	0.9883	4.798×10^{-9}

Table 4. Thermodynamic constants for POD adsorption ontoAlg–GG beads.

System	ΔH° (kJ mol^{-1})	ΔS° (J mol^{-1} K^{-1})
S2	−11.42	−94.11
S3	−2.49	−53.30

expression that can simulate both Langmuir and Freundlich behaviours (Jeppu and Clement, 2012).

Figure 3 shows the fitting of the experimental data according to the three adsorption models proposed for the systems S2 and S3. Besides, Table 3 shows the adsorption values obtained from the fitting of the data to the Freundlich, Langmuir and LF isotherm models.

The statistical analysis of the error function shows that the equation that best fitted the data for both system is the Freundlich model (see Table 3), this occurs at the two temperatures assayed.

Thermodynamics studies

Adsorption thermodynamics of POD adsorption by Alg–GG beads were studied at different temperatures (279.15 K and 294.15 K).Thermodynamic constants for POD adsorption by Alg–GG beads for S2 and S3 are shown in Table 4.

The adsorption process was temperature dependent as shown in Figure 3 and, it was found that increasing the temperature induced a significant decrease in the adsorption process in agreement with the negative ΔH found for both systems. The negative value of ΔH indicated that the adsorption process was exothermic in nature; this is consequence of the bound formation between the POD and the electrical charged groups of the matrix (COOH) and dipole–dipole interaction between the polar groups of POD and the polysaccharides chains. Judging by the low values ΔH observed, the interaction can be considered as a poor electrostatic content.

Net chemical adsorption is associated to ΔH values of 40–80 kJ/mol, so our results suggest the presence of a physical interaction model as shown in Table 4. Negative ΔS implies that the whole system is more ordered after the adsorption due to the bound formation. The negative ΔS values indicate that randomness decreases at the solid–solution interface during the POD sorption onto Alg–GG. The negative ΔH and ΔS values suggest that enthalpy contributes more than entropy in negative ΔG values. Similar results have been reported for the biosorption of dyes and heavy metals onto algae (Dotto et al., 2012).

The temperature increase induced a decrease in the negative entropy value suggesting an increase in the disorder of the system, this finding should be assigned to the loss of water molecules which interact with the OH polysaccharides groups by temperature effect.

At ambient temperature S2 showed a greater capacity to adsorb the enzyme than S3, probably due to the larger separation between the polysaccharide chain caused by S2 low alginate content. At low temperature the inverse effect was observed; the increase in the alginate induces an increase in the adsorption of protein. These results suggest that the temperature can induce a modification in the distance between the polysaccharide chains in a significant manner, facilitating the penetration of the enzyme molecule to the interior of the matrix.

Adsorbed POD activity measured

With the goal to verify the effective bound of the enzyme to the matrix, activity measures were done using the matrix with adsorbed enzyme. The catalytic activity of the immobilized enzyme remains constant over time. Besides from the mass balance of the system the measured value correspond to the results obtained using the depletion method (data not shown).

Conclusions

The possibility of using Alg–GG matrices cross-linked by epichlorohydrin for the adsorption of a vegetal peroxidase was examined in this work. The capacity of adsorption showed to be optimal at pH 4.0 for matrices with 1.0% and 1.5% of alginate (w/v) and 0.5% GG (w/v). At this pH the carboxyl groups of alginate have negative electrical groups, which interact with the positively groups of POD, when the pH was increased, the adsorption process decreased, being null at pH 6.0. The kinetics of the sorption process showed fitted to a first- and second-order-process, however, the analysis of the data suggests that two process are involved in the adsorption mechanism: a diffusion of the protein from the solution to the surface of the matrix and secondly the intra particle diffusion. Thermodynamic analysis of the data showed low values of ΔS and ΔH, in agreement with the enzyme–matrix interaction that occurs mainly by a physical mechanism. The POD adsorbed onto the matrix maintained its enzyme activity entirely; this is an important finding because it opens the possibility to use this enzyme as an immobilized catalyser in a bioreactor. This study demonstrates that Alg–GG matrices can be used as a potential adsorbent of protein; the advantage of this system is being eco-friendly and having non-expensive properties.

Acknowledgements

Ana Silva thanks the EC for her fellowship in IPROBYQ-Rosario, Argentine.

Declaration of Conflicting Interests

The author(s) declared no potential conflicts of interest with respect to the research, authorship, and/or publication of this article.

Funding

The author(s) disclosed receipt of the following financial support for the research, authorship, and/or publication of this article: FonCyT, Projects PICT 2013–271 – Argentina Innovator 2020 and Biotechnologies to Valorize the regional food Biodiversity in Latin America – Marie Curie Actions – IRSES Project number 611493 – European Community.

References

Bai J, Fan F, Wu X, et al. (2013) Equilibrium, kinetic and thermodynamic studies of uranium biosorption by calcium alginate beads. *Journal of Environmental Radioactivity* 126: 226–231.

Chiou M-S, Ho P-Y and Li H-Y (2004) Adsorption of anionic dyes in acid solutions using chemically cross-linked chitosan beads. *Dyes and Pigments* 60(1): 69–84.

Daly MM and Knorr D (1988) Chitosan–alginate complex coacervate capsules: Effects of calcium chloride, plasticizers, and polyelectrolytes on mechanical stability. *Biotechnology Progress* 4(2): 76–81.

Daneshvar E, Kousha M, Jokar M, et al. (2012) Acidic dye biosorption onto marine brown macroalgae: Isotherms, kinetic and thermodynamic studies. *Chemical Engineering Journal* 204–206: 225–234.

Doğan M and Alkan M (2003) Adsorption kinetics of methyl violet onto perlite. *Chemosphere* 50(4): 517–528.

Dotto GL, Lima EC and Pinto LAA (2012) Biosorption of food dyes onto Spirulina platensis nanoparticles: Equilibrium isotherm and thermodynamic analysis. *Bioresource Technology* 103(1): 123–130.

Gadd GM (2009) Biosorption: Critical review of scientific rationale, environmental importance and significance for pollution treatment. *Journal of Chemical Technology & Biotechnology* 84(1): 13–28.

Gotoh T, Matsushima K and Kikuchi K (2004) Preparation of alginate-chitosan hybrid gel beads and adsorption of divalent metal ions. *Chemosphere* 55(1): 135–140.

Jeppu GP and Clement TP (2012) A modified Langmuir–Freundlich isotherm model for simulating pH-dependent adsorption effects. *Journal of Contaminant Hydrology* 129–130: 46–53.

Kulkarni AR, Soppimath KS, Aminabhavi TM, et al. (2000) Glutaraldehyde crosslinked sodium alginate beads containing liquid pesticide for soil application. *Journal of Controlled Release* 63(1–2): 97–105.

Lee KY and Mooney DJ (2012) Alginate: Properties and biomedical applications. *Progress in Polymer Science* 37(1): 106–126.

López-Morales J, Sánchez-Rivera D, Luna-Pineda T, et al. (2013) Entrapment of tyre crumb rubber in calcium-alginate beads for triclosan removal. *Adsorption Science & Technology* 31(10): 931–942.

Luo C, Wei R, Guo D, et al. (2013) Adsorption behavior of MnO_2 functionalized multi-walled carbon nanotubes for the removal of cadmium from aqueous solutions. *Chemical Engineering Journal* 225: 406–415.

Mohammadi N, Khani H, Gupta VK, et al. (2011) Adsorption process of methyl orange dye onto mesoporous carbon material–kinetic and thermodynamic studies. *Journal of Colloid and Interface Science* 362(2): 457–462.

Mudgil D, Barak S and Khatkar B (2014) Guar gum: processing, properties and food applications – A review. *Journal of Food Science and Technology* 51(3): 409–418.

Paques JP, van der Linden E, van Rijn CJ, et al. (2014) Preparation methods of alginate nanoparticles. *Advances in Colloid and Interface Science* 209: 163–171.

Pardo R, Herguedas M, Barrado E, et al. (2003) Biosorption of cadmium, copper, lead and zinc by inactive biomass of Pseudomonas Putida. *Analytical and Bioanalytical Chemistry* 376(1): 26–32.

Rangabhashiyam S, Anu N, Nandagopal MG, et al. (2014) Relevance of isotherm models in biosorption of pollutants by agricultural byproducts. *Journal of Environmental Chemical Engineering* 2(1): 398–414.

Roy I, Sardar M and Gupta MN (2005) Cross-linked alginate–guar gum beads as fluidized bed affinity media for purification of jacalin. *Biochemical Engineering Journal* 23(3): 193–198.

Somers WAC, Kutsch Lojenga A, Bonte A, et al. (1993) Alginate-starch co-polymers and immobilized starch as affinity adsorbents for amylase. *Biotechnology and Applied Biochemistry* 18: 9–24.

Spelzini D, Farruggia B and Picó G (2011) Purification of chymotrypsin from pancreas homogenate by adsorption onto non-soluble alginate beads. *Process Biochemistry* 46(3): 801–805.

Vadivelan V and Kumar KV (2005) Equilibrium, kinetics, mechanism, and process design for the sorption of methylene blue onto rice husk. *Journal of Colloid and Interface Science* 286(1): 90–100.

Woitovich Valetti N and Picó G (2016) Adsorption isotherms, kinetics and thermodynamic studies towards understanding the interaction between cross-linked alginate-guar gum matrix and chymotrypsin. *Journal of Chromatography B* 1012–1013: 204–210.

Yoon S-J, Chu D-C and Raj Juneja L (2008) Chemical and physical properties, safety and application of partially hydrolized guar gum as dietary fiber. *Journal of Clinical Biochemistry and Nutrition* 42(1): 1–7.

Zhang S, Xu F, Wang Y, et al. (2013) Silica modified calcium alginate–xanthan gum hybrid bead composites for the removal and recovery of Pb(II) from aqueous solution. *Chemical Engineering Journal* 234: 33–42.